CHROM. 4405

AN EQUILIBRIUM THEORY FOR RARE-EARTH SEPARATION BY DISPLACEMENT DEVELOPMENT

F. HELFFERICH
Shell Development Company, Emeryville, Calif. 94608 (U.S.A.)

AND

D. B. JAMES*
Nuclear Materials and Equipment Corporation, Apollo, Pa. 15613 (U.S.A.)

(Received September 29th, 1969)

SUMMARY

A general equilibrium theory of chromatography is applied to the separation of rare earths by displacement development on a cation exchanger. The essential premises are local equilibrium, uniform sorbent properties, plug flow, absence of axial diffusion, stoichiometric exchange, and constant separation factors. Both development of a preadsorbed uniform band with a chelating agent and operation with chelation prior to loading are considered. The theory yields the distances and times required for resolution of any component from any other was well as the mobile-phase and stationary phase compositions at any point and time during development. Application of the theory to the separation of a fifteen-component rare-earth mineral, euxenite, illustrates the method.

INTRODUCTION

A highly successful process for preparative commercial separation of rare earths in ton quantities with high purity is displacement development with a chelating agent on a cation exchanger[1,2]. The characteristic and well-known features of this type of separation are that the mixture to be separated travels as a band of constant width, being displaced by a chelating development agent and itself displacing a retaining agent with which the column was presaturated; on its way through the column (or through a number of columns in series) the species within the band sort themselves out into individual zones of one species each, which all travel at the same rate and follow one another without interval. In practice, finite mass-transfer rates and unavoidable disturbances cause some overlap between the final zones, but under the simplifying premises usually employed the theory gives ideally sharp boundaries between the zones. A typical operation is with an ammonium-EDTA buffer as the development agent on a strong-acid cation exchanger with Cu^{2+} as the retaining ion,

* The contribution of D. B. JAMES to this work was supported by Michigan Chemical Corporation, St. Louis, Mich., U.S.A.

as developed by SPEDDING AND POWELL and their associates[1,3,4], to whose publications we refere for chemical mechanism, equipment, and practical details.

The development behavior is illustrated in Fig. 1 for the separation of a preadsorbed uniform band of a binary mixture. As development proceeds, the zone having the composition of the original mixture shrinks and eventually disappears, while zones of the two pure components grow on either side, all within the traveling band of constant length. The broken lines, superimposed on the column pictures, trace the traveling boundaries between the zones of different compositions.

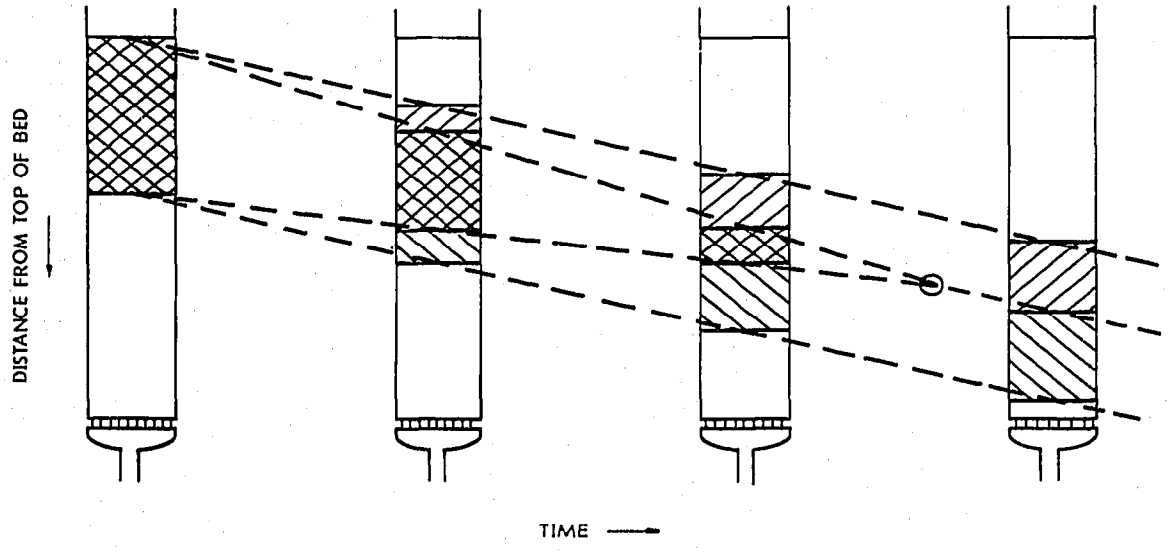

Fig. 1. Separation of binary mixture (schematic). (From D. B. JAMES, J. E. POWELL AND H. R BURKHOLDER[9].)

For optimum design, a knowledge of the distance and time a given mixture must travel to be resolved is obviously of key importance. Previous theoretical treatments, by SILLÉN[5] and SPEDDING, POWELL *et al.*[4,6–9], have given solutions for separations of binary and ternary mixtures but are not readily extended to more complex cases. A recent general theory of multicomponent chromatography under arbitrary initial and influent conditions[10], however, comprises displacement development as a special case and can be applied to provide the desired extension to any number of components, as will be shown here.

Computations with the formulas which follow are straightforward but become lengthy for systems with many components. For these a computer program that tabulates and plots the results has been made available[11]. The results calculated by this program for a fifteen-component separation will be shown here as an example.

Space limitations forbid us to give more than the mere outlines of derivations and proofs. For details reference to the original theory[10] must be made.

PREMISES

The usual assumptions of "equilibrium theories" of chromatography are made, namely, existence of local equilibrium at any point and time, uniform sorbent properties, plug flow, and absence of axial diffusion. We assume, moreover, that ion exchange is stoichiometric (*i.e.*, without change in total number of equivalents in either phase) and that the separation factors are constant. Volume changes of the ion exchanger are disregarded, and for convenience we only consider operations with a column of uniform cross section and with constant composition and flow rate of the development agent. These assumptions are essentially the same as in the earlier theoretical treatments, except that the premise of low solution concentration relative to the concentration in the ion exchanger, made by SPEDDING, POWELL *et al.*, is not needed.

Theories based on these premises are unrealistic in that they yield ideally sharp boundaries between the various zones of different compositions, boundaries that in actual operation are slightly diffuse. However, since practical rare-earth separations are conducted so that diffuse overlaps between zones are small compared to the band and zone widths, this idealization does not significantly impair the utility of the theory.

NOTATION AND DEFINITIONS

We shall consider the separation of an arbitrary n-component mixture. The species are numbered 1, 2, ..., n in the order of decreasing affinity for the ion exchanger in the presence of the chelating agent. Concentrations are given as equivalent ionic fractions x_i in the liquid and y_i in the ion exchanger ($i = 1, \ldots, n$). Thus, by definition

$$\sum_{i=1}^{n} x_i = 1 \quad \text{and} \quad \sum_{i=1}^{n} y_i = 1 \tag{1}$$

at any point in the band. Separation factors α_{1i} relative to the reference species 1 are defined as

$$\alpha_{1i} \equiv \frac{y_1 \, x_i}{x_1 \, y_i} \qquad (i = 1, \ldots, n) \tag{2}$$

(According to POWELL AND SPEDDING[4], these factors are virtually equal to the ratios of the stability constants of the respective chelates, chelation being the almost exclusive cause of selectivity.)

For mathematical convenience and greater generality, the derivations make use of a normalized and adjusted time variable, τ, defined as

$$\tau \equiv (tu_0 - z)C/\bar{C} \tag{3}$$

where t is the true time (say, in seconds), u_0 is the linear liquid flow rate (in cm/sec), z is the distance from the top of the bed (in cm), and C and $\bar{C}$ are the total concentrations (sums of concentrations of all components, in ionic equivalents per unit volume of column) in the liquid and ion exchanger, respectively. (The "adjustment" by $-z$ in eqn. (3) is the mathematically most convenient way of removing the premise $C \ll \bar{C}$ adopted in most earlier theories. Note that the adjusted time has the dimension of a length.)

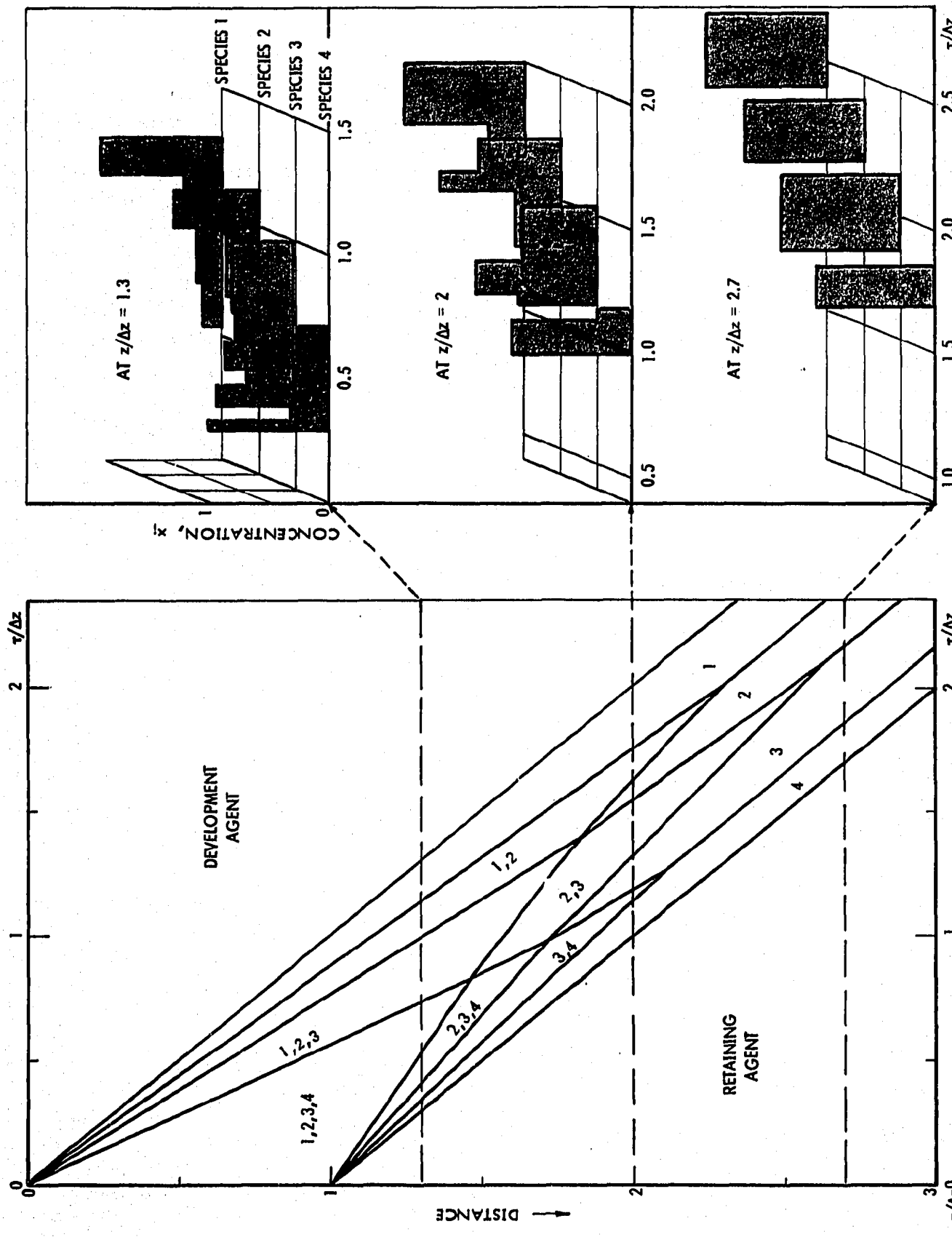

Fig. 2. Distance–time diagram and concentration histories at three different column levels for quaternary separation by development of uniform initial band. (Calculated for initial composition $\nu_1^0 = 0.298$, $\nu_2^0 = 0.239$, $\nu_3^0 = 0.304$, $\nu_4^0 = 0.159$ and separation factors $\alpha_{21} = 1.40$, $\alpha_{32} = 2.05$

The adjusted velocity, u_Δ, of a boundary between zones of different compositions is defined as

$$u_\Delta \equiv \partial z/\partial\tau|_\Delta \tag{4}$$

where Δ symbolizes the boundary. The definition of τ has been chosen so that the adjusted velocity of the rare-earth band (*i.e.*, of its front and rear boundaries) is unity.

OUTLINE OF THEORY

Distance–time diagrams

The derivations make use of geometrical constructions in "distance–time diagrams", which show the trajectories of boundaries between zones of different compositions. For easier mental translation into and from actual column operation, which is usually downflow, distance from the top of the bed is plotted downward; with the column pictures removed, Fig. 1 would thus immediately give a distance–time diagram. A diagram for a four-component case is shown in Fig. 2. The resolution distances and times, ultimately sought by the theory, are the coordinate values of the points at which trajectories intersect, and can thus be calculated once the velocities of the boundaries (trajectory slopes) are known.

Boundary velocities

A simple material-balance argument (amount entering minus amount leaving a column segment equals net change in content of segment), the starting point of theory in almost any text on chromatography, shows that a concentration step of an arbitrary species i advances at the true velocity $u_0\Delta C_i/(\Delta C_i + \Delta\bar{C}_i)$, where ΔC_i and $\Delta\bar{C}_i$ are the concentration differences in the liquid and ion exchanger, respectively, across the step. (The usual equations differ in that they involve the fractional phase volumes; these cancel if, as is done here, the concentrations are expressed per unit volume of column rather than of the respective phase.) Conversion to adjusted velocity and equivalent fractions gives

$$u_\Delta = \Delta x_i/\Delta y_i \tag{5}$$

(where Δx_i and Δy_i are the differences across the step), as can be verified by eqns. (3) and (4). This relation holds for any species i.

Coherence

In multicomponent systems, a boundary between zones of different composition usually involves concentration variations of any number of species. If the boundary is to travel without splitting up into separate concentration steps, it is evident that eqn. (5) *must apply to all species simultaneously*, since the concentration steps of different species would otherwise travel at different velocities. Accordingly:

$$\Delta x_1/\Delta y_1 = \Delta x_2/\Delta y_2 = \ldots = \Delta x_n/\Delta y_n \tag{6}$$

for any given boundary. In the general theory[10], boundaries that meet this criterion are called *coherent*, and it is shown that and how coherent boundaries evolve from any arbitrary initial conditions. In the present case, the two initial composition

steps, at the front and rear of the uniform initial band, are noncoherent and break up into sets of coherent boundaries. Similarly, where two coherent boundaries cross, there is for an instant a noncoherent step, which immediately breaks up again into two coherent boundaries. All earlier theories have implied without proof that coherent boundaries are indeed formed.

h-Transformation and H-function roots

Except for the zone of the original mixture and those at the extreme rear and front of the band, where only species 1 and n, respectively, are present, the various transient compositions are not known beforehand. Eqn. (5) by itself is therefore not sufficient to calculate boundary velocities. This difficulty is best overcome with the so-called *h-transformation*, by which the set of composition variables $x_1,\ldots,x_n$ or $y_1,\ldots,y_n$ is replaced by a new set $h_1,\ldots,h_{n-1}$. [Only $n-1$ variables are needed since, in view of eqn. (1), only $n-1$ concentrations x_i or y_i can be varied independently.] The advantage of the new variables is that all boundary velocities and other quantities of interest can be calculated directly from the set of h_i *of the initial mixture alone*, without the need for computing intermediate compositions or properties.

The h_i are defined as the $n-1$ roots in h (or reciprocals of the roots in $1/h$) of the so-called "H-function":

$$\sum_{i=1}^{n} \left[\prod_{\substack{j=1 \\ j\neq i}}^{n} (h-\alpha_{1j})x_i \right] = 0 \qquad (7)$$

or

$$\sum_{i=1}^{n} \left[\prod_{\substack{j=1 \\ j\neq i}}^{n} \left(\frac{1}{h}-\frac{1}{\alpha_{1j}}\right) y_i \right] = 0 \qquad (8)$$

It can be readily verified that compositions $x_1,\ldots,x_n$ and $y_1,\ldots,y_n$ in equilibrium with one another give the same set of H-function roots. The roots are all real and fall into the intervals

$$\alpha_{1i} \leq h_i \leq \alpha_{1,i+1} \qquad (i = 1,\ldots,n-1) \qquad (9)$$

For each species k absent from the respective composition, the polynomial (7) or (8) has a "trivial root" $h = \alpha_{1k}$. Thus

$$\begin{array}{lll} h_1 = 1 & \text{if } x_1 = 0, y_1 = 0 & \\ h_{i-1} = \alpha_{1i} \text{ or } h_i = \alpha_{1i} & \text{if } x_i = 0, y_i = 0 & (1 < i < n) \\ h_{n-1} = \alpha_{1n} & \text{if } x_n = 0, y_n = 0 & \end{array} \qquad (10)$$

The other, nontrivial roots are more conveniently calculated from the relations

$$\sum_{i=1}^{n} \frac{x_i}{h-\alpha_{1i}} = 0 \quad \text{or} \quad \sum_{i=1}^{n} \frac{y_i}{1/h-1/\alpha_{1i}} = 0 \qquad (11)$$

obtained when eqn. (7) is divided by $\prod_{j=1}^{n} (h-\alpha_{1j})$, or eqn. (8) by $\prod_{j=1}^{n} (1/h-1/\alpha_{1j})$.

The roots are readily found by standard numerical procedures, since the functions in

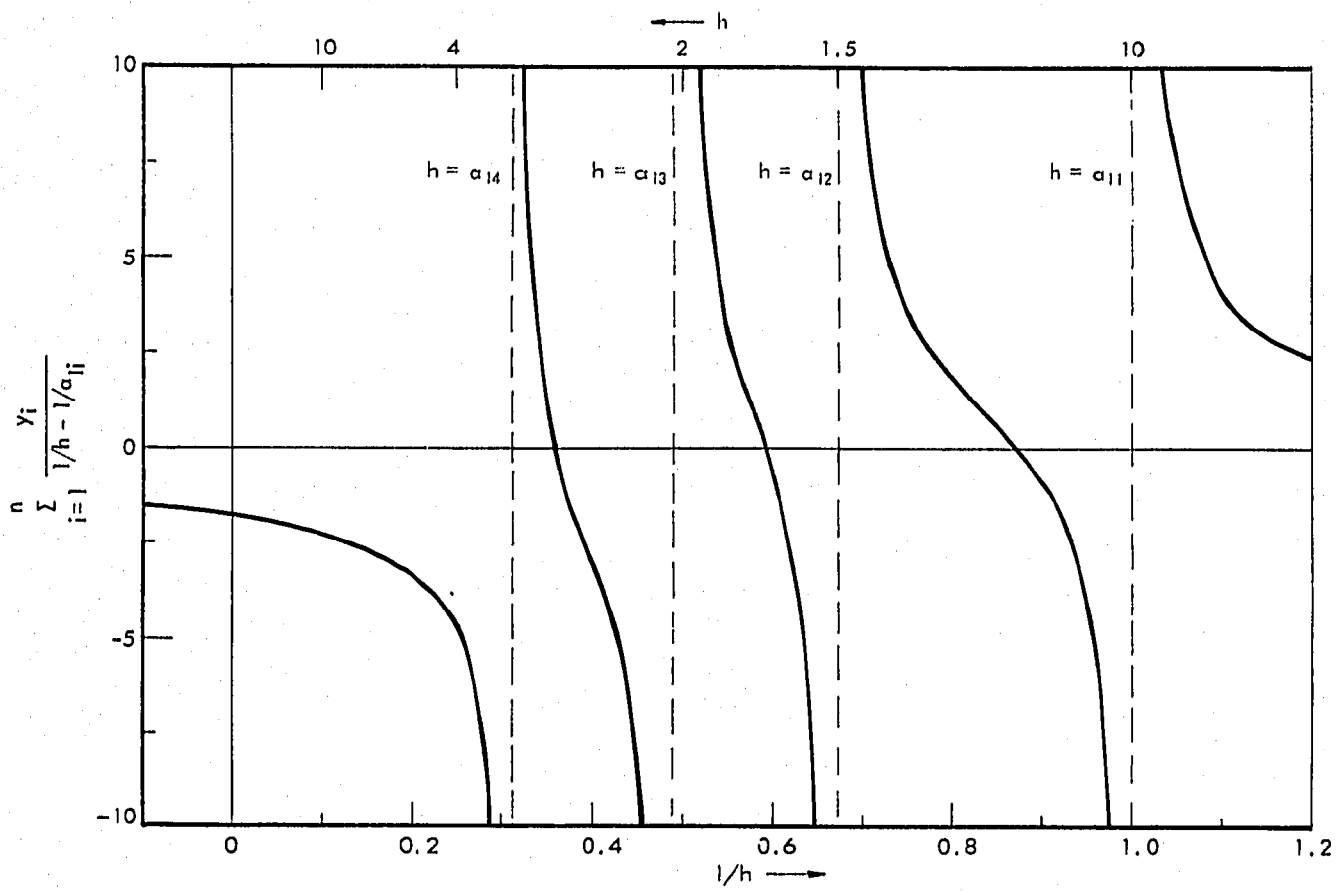

Fig. 3. Function $\sum_{i=1}^{n} y_i/(1/h - 1/a_{1i})$ *versus* $1/h$. (Calculated for same composition and separation factors as in Fig. 2.)

h are single-valued and monotonic between their poles at the various $h = a_{1i}$. An example of this behavior is shown in Fig. 3.

For two and three components, the roots can be given conveniently in an explicit form. Eqn. (11), solved for h, gives for two-component compositions

$$h = \alpha_{12}x_1 + x_2 \qquad \text{and} \qquad h = \frac{1}{y_1/\alpha_{12} + y_2} \tag{12}$$

and for three-component compositions

$$h_{1,2} = \tfrac{1}{2}\left[A \pm (A^2 - 4B)^{\frac{1}{2}}\right] \quad \text{and} \quad h_{1,2} = \frac{2}{\bar{A} \pm (\bar{A}^2 - 4\bar{B})^{\frac{1}{2}}} \tag{13}$$

where

$$A \equiv 1 - x_1 + \alpha_{12}(1 - x_2) + \alpha_{13}(1 - x_3)$$
$$B \equiv \alpha_{12}\alpha_{13}x_1 + \alpha_{13}x_2 + \alpha_{12}x_3$$
$$\bar{A} \equiv 1 - y_1 + (1 - y_2)/\alpha_{12} + (1 - y_3)/\alpha_{13}$$
$$\bar{B} \equiv y_1/\alpha_{12}\alpha_{13} + y_2/\alpha_{13} + y_3/\alpha_{12}$$

For the converse transformation, to obtain concentrations x_i or y_i from given sets of H-function roots, explicit equations can be written for any number of components:

$$x_j = \prod_{i=1}^{n-1}(h_i - a_{1j}) \Big/ \prod_{\substack{i=1 \\ i \neq j}}^{n} (a_{1i} - a_{1j}) \qquad (14)$$

$$(j = 1, \ldots, n)$$

$$y_j = \prod_{i=1}^{n-1}\left(\frac{1}{h_i} - \frac{1}{a_{1j}}\right) \Big/ \prod_{\substack{i=1 \\ i \neq j}}^{n}\left(\frac{1}{a_{1i}} - \frac{1}{a_{1j}}\right) \qquad (15)$$

These equations can be obtained as the solutions of the eqns. (11) with h_1, h_2, ..., h_{n-1} consecutively substituted for h.

Properties and behavior of H-function roots

Two of the properties of the H-function roots, examined in detail in the general theory, are of special importance in the present case. The first one is that *only one root varies across any coherent boundary*, and the second, that any boundary in the course of development is a root variation, propagated across the distance–time plane, that *existed initially or was introduced as an influent composition change*. A corollary of the second rule is that *no root values other than those of the initial and influent compositions will occur anywhere at any time*. An abbreviated proof of the first rule, applicable to the present case, is given in the Appendix, where it is also shown that the adjusted velocity of a coherent composition step with h_k as the varying root is given by

$$u_\Delta = h_k' \, h_k'' \prod_{\substack{i=1 \\ i \neq k}}^{n-1} h_i \Big/ \prod_{i=1}^{n} a_{1i} \qquad (16)$$

where h_k' and h_k'' are the values of h_k on the two sides of the step. For the more complex proof of the conservation properties of the roots reflected in the second rule we must refer to the original theory[10].

The two initial composition steps, at the front and rear of the uniform initial band, involve variations of all H-function roots and thus are noncoherent. Upon development they break up into sets of coherent boundaries each involving variation of one root only. Within each set, the boundaries are in the sequence of increasing index numbers of their variable roots (seen in the direction of flow), since eqn. (16) with condition (9) gives the higher velocity for the boundary with variable root of higher index number. In the distance–time plane, each of the sets of boundaries appears as a bundle of trajectories having a common point of origin. The trajectories of the two bundles cross: each trajectory of a root variation Δh_k of the upstream bundle crosses all those of variations Δh_1, Δh_2, ..., Δh_{k-1} of the downstream bundle and eventually merges with that of Δh_k of the downstream bundle; the last is a merger rather than a cross-over because a single coherent boundary is formed from two coherent boundaries if these involve variations of the *same* root. The resulting overall trajectory pattern in the distance–time plane is shown schematically in Fig. 4.

The root values for the uniform initial zone can be calculated from its composition x_1°, ..., x_n° or y_1°, ..., y_n° from eqn. (11) and will be designated h_1°, ...,

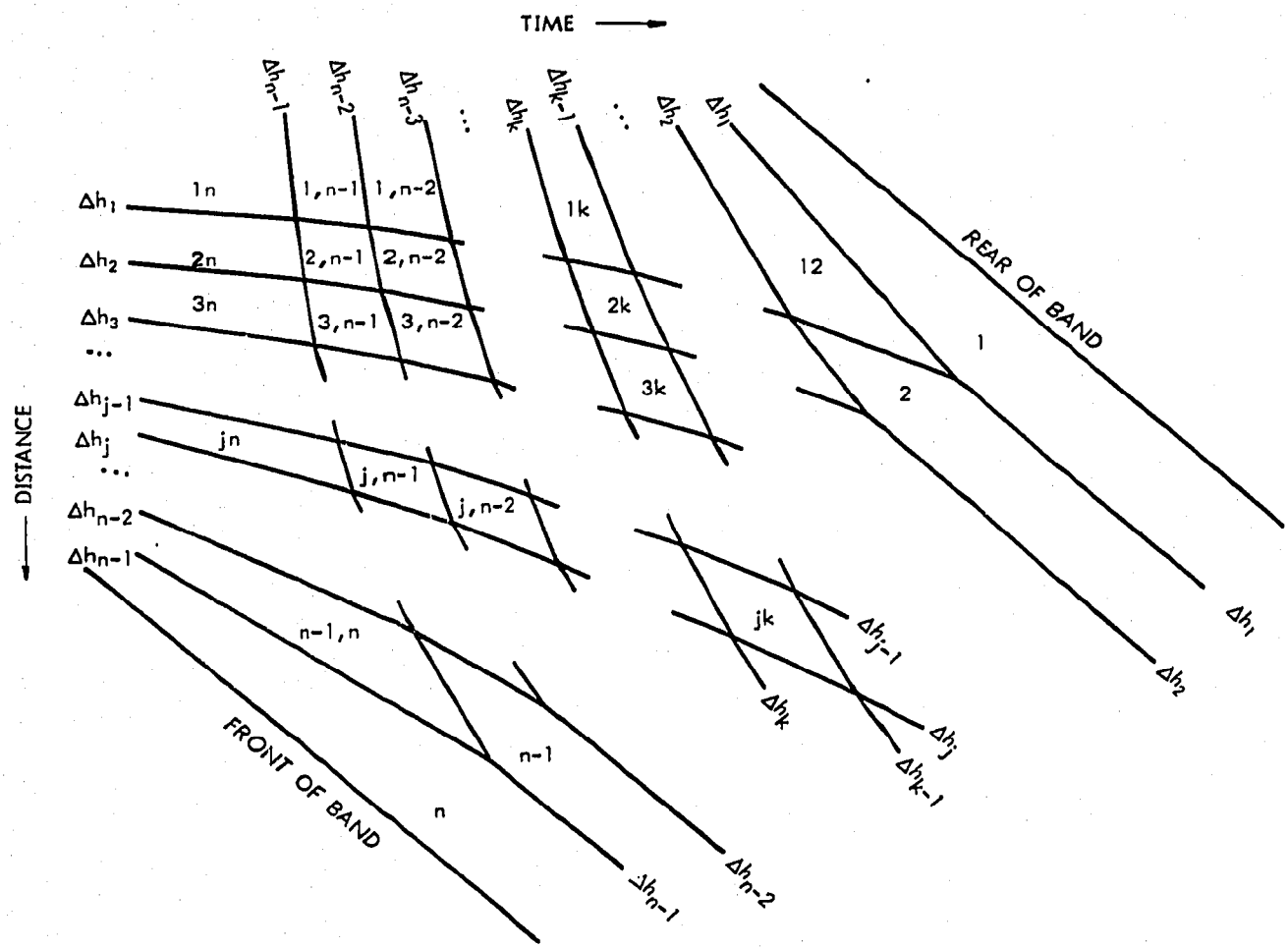

Fig. 4. Pattern of trajectories in distance–time plane (schematic). (Adapted from HELFFERICH AND KLEIN[10].)

$h_n°_{-1}$. The root values at the extreme rear and front of the traveling band, where only species 1 and n, respectively, are present, are readily obtained from condition (10). At the rear, the absence of species 2, ..., n gives rise to the $n-1$ "trivial" roots

$$h_1 = \alpha_{1,i+1} \qquad (i = 1, \ldots, n-1) \tag{17}$$

the index numbers being dictated by condition (9). Similarly, at the front, the absence of species 1, ..., $n-1$ gives rise to the $n-1$ trivial roots

$$h_i = \alpha_{1i} \qquad (i = 1, \ldots, n-1) \tag{18}$$

Thus, any root h_k varies from $\alpha_{1,k+1}$ to $h_k°$ across the Δh_k trajectory of the upstream bundle, and from $h_k°$ to α_{1k} across the Δh_k trajectory of the downstream bundle; the region of $h_k°$ narrows with progressing development and disappears when the two Δh_k trajectories merge.

Compositions of the zones

The composition of all the zones in the distance–time plane can now be calculated

from the roots h_i° of the initial mixture. We shall characterize the various zones by double numbers, jk referring to the zone between the trajectories of Δh_{j-1} and Δh_j of the downstream bundle and those of Δh_{k-1} and Δh_k of the upstream bundle ($j < k$). Using this convention, the jk zone is downstream of the trajectories of all Δh_i with $i < j$ of both bundles, upstream of the trajectories of all Δh_i with $i > k$ of both bundles, and between the upstream-bundle and downstream-bundle trajectories of all Δh_i with $j \leq i \leq k$. With the variations of the root values across the respective trajectories as noted earlier, the set of roots in the jk zone then is

$$\begin{aligned} h_i &= \alpha_{1i} && (i = 1, \ldots, j-1) \\ h_i &= h_i^\circ && (i = j, \ldots, k-1) \\ h_i &= \alpha_{1,i+1} && (i = k, \ldots, n-1) \end{aligned} \tag{19}$$

and, as conditions (10) show, only species $j, \ldots, k$ are present in the zone. The concentrations of these species can be calculated from eqns. (14) or (15), which give, with the appropriate substitutions,

$$x_l = \prod_{i=j}^{k-1}(h_i^\circ - \alpha_{1l}) \Bigg/ \prod_{\substack{i=j \\ i \neq l}}^{k} (\alpha_{1i} - \alpha_{1l}) \qquad (l = j, \ldots, k) \tag{20}$$

$$y_l = \prod_{i=j}^{k-1}\left(\frac{1}{h_i^\circ} - \frac{1}{\alpha_{1l}}\right) \Bigg/ \prod_{\substack{i=j \\ i \neq l}}^{k} \left(\frac{1}{\alpha_{1i}} - \frac{1}{\alpha_{1l}}\right)$$

Boundary velocities

The adjusted velocities of all boundaries can be calculated with equal ease from the H-function roots of the initial mixture. All that is needed is the substitution of the appropriate root values into the general equation (16). For the upstream trajectory bundle, generated by the composition step at the rear of the uniform initial band, one finds that the adjusted velocity of the variation Δh_k of the arbitary root h_k at the zone jk (*i.e.*, between the Δh_{j-1} and Δh_j trajectories of the downstream bundle) is

$$u_\Delta = \prod_{i=j}^{k} (h_i^\circ/\alpha_{1i}) \tag{21}$$

Similarly, one finds for the adjusted velocity of the variation Δh_j of the downstream bundle at the jk zone (*i.e.*, between the Δh_{k-1} and Δh_k trajectories of the upstream bundle):

$$u_\Delta = \prod_{i=j}^{k-1} (h_i^\circ/\alpha_{1,i+1}) \tag{22}$$

As Fig. 4 has shown, the Δh_k trajectory of the upper bundle crosses, in this sequence, those of $\Delta h_1, \Delta h_2, \ldots, \Delta h_{k-1}$ of the lower bundle, and the Δh_j trajectory of the lower bundle crosses, in this sequence, those of $\Delta h_{n-1}, \Delta h_{n-2}, \ldots, \Delta h_{j+1}$ of the upper bundle. Accordingly, the products in eqns. (21) and (22) lose one of their factors h_1°/α_{11}, h_2°/α_{12}, ... and $h_{n-1}^\circ/\alpha_{1n}$, $h_{n-2}^\circ/\alpha_{1,n-1}$, ... with each successive cross-over. Since condition (9) requires

$$h_i^\circ/\alpha_{1,i+1} < 1 < h_i^\circ/\alpha_{1i} \qquad (i = 1, \ldots, n-1) \tag{23}$$

the adjusted velocities of all boundaries of the upper bundle are larger than unity and decrease with each cross-over, whereas those of the lower bundle are all smaller than unity and increase with each cross-over. The adjusted velocity becomes unity when the two Δh_k trajectories (or Δh_j trajectories) of the two bundles finally merge.

Resolution distances and times

A glance at the distance–time diagram reveals that the zone jk is the last and farthest downstream to contain species j and k in the presence of one another. The development distance (*i.e.*, bed length) and adjusted time, z_{jk} and τ_{jk}, required for the resolution of these two species are thus given as the z and τ coordinate values of the point at which this zone disappears, that is, of the "southeast" corner of the zone in the distance–time diagram. Given the composition of the initial mixture and the width of its band, all resolution distances and times can thus be calculated in a straightforward manner by construction of the trajectory grid from the given points of origin of the bundles with the use of eqns. (21) and (22) for the trajectory slopes. The results of this calculation are listed in Table I. Derivations are provided in the Appendix.

Table I gives formulas for two types of operation, namely, development of a uniform initial band as in Figs. 1 and 2, and operation with chelation of the mixture prior to its introduction into a column initially loaded with only the retaining ion, as

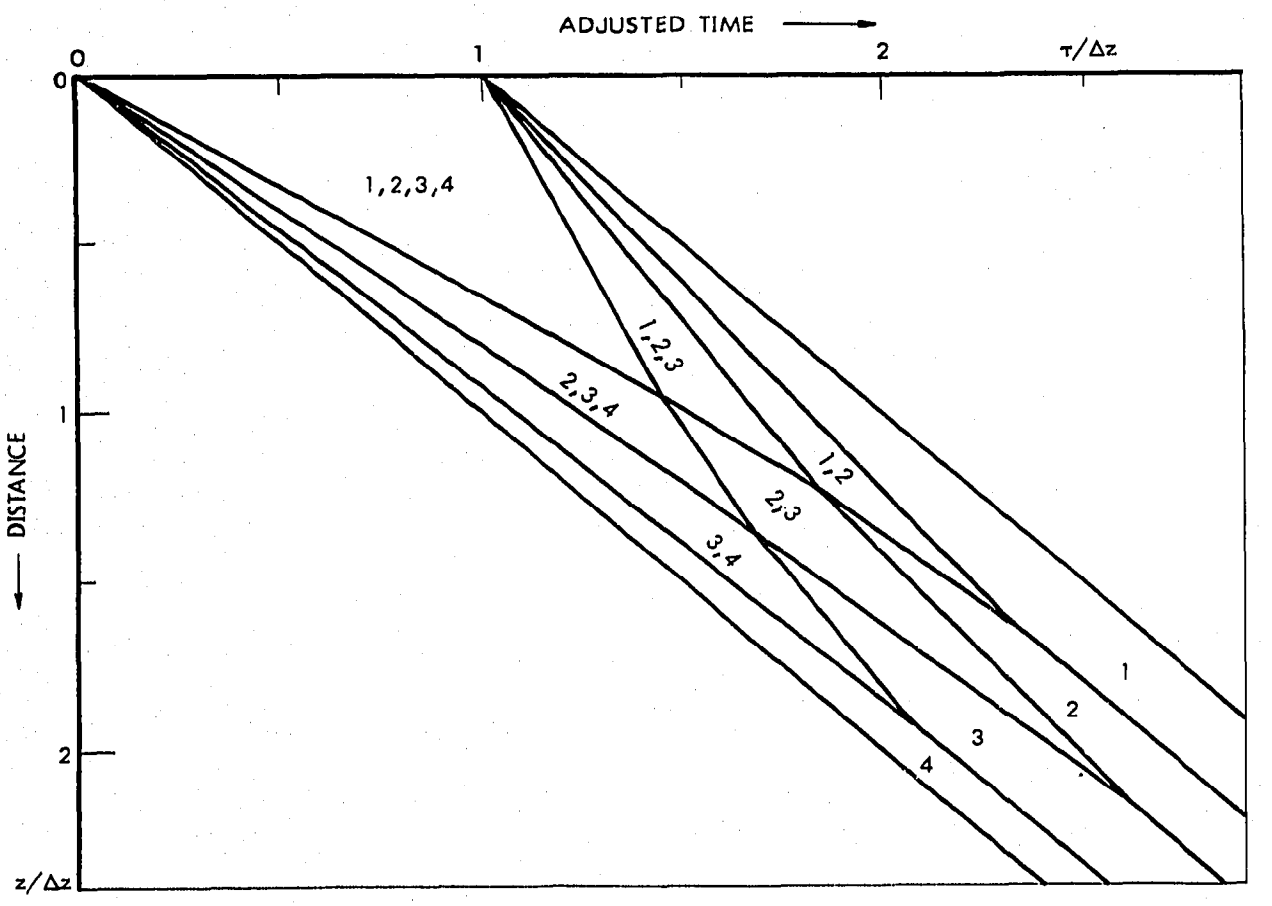

Fig. 5. Distance–time diagram for quaternary separation with chelation prior to loading. (Calculated for same original mixture and separation factors as in Fig. 2.)

TABLE I

DISTANCES AND ADJUSTED TIMES FOR RESOLUTION

Development of uniform initial band	*Operation with chelation prior to loading*
Binary separations	
$z_{12} = \frac{\alpha_{12}}{\alpha_{12}-1}\Delta z$	$z_{12} = \left(\frac{1}{\alpha_{12}-1} + x_1^\circ\right)\Delta z$
$\tau_{12} = \left(\frac{1}{\alpha_{12}-1} + y_2^\circ\right)\Delta z$	$\tau_{12} = \frac{\alpha_{12}}{\alpha_{12}-1}\Delta z$
Ternary separations	
$z_{13} = \frac{\alpha_{13}}{\alpha_{13}-1}\Delta z$	$z_{13} = \frac{\alpha_{13}x_1^\circ + \alpha_{12}x_2^\circ + x_3^\circ}{\alpha_{13}-1}\Delta z$
$\tau_{13} = \frac{y_1^\circ + \alpha_{23}y_2^\circ + \alpha_{13}y_3^\circ}{\alpha_{13}-1}\Delta z$	$\tau_{13} = \frac{\alpha_{13}}{\alpha_{13}-1}\Delta z$
$z_{12} = \frac{\alpha_{12}\alpha_{13}(h_2^\circ-1)}{h_2^\circ(\alpha_{12}-1)(\alpha_{13}-1)}\Delta z$	$z_{12} = \frac{h_1^\circ(h_2^\circ-1)}{(\alpha_{12}-1)(\alpha_{13}-1)}\Delta z$
$\tau_{12} = \frac{\alpha_{12}\alpha_{13}(h_2^\circ-1)}{h_1^\circ h_2^\circ(\alpha_{12}-1)(\alpha_{13}-1)}\Delta z$	$\tau_{12} = \left(1 + \frac{h_2^\circ-1}{(\alpha_{12}-1)(\alpha_{13}-1)}\right)\Delta z$
$z_{23} = \left(1 + \frac{\alpha_{13}(\alpha_{13}-h_1^\circ)}{h_1^\circ(\alpha_{13}-1)(\alpha_{13}-\alpha_{12})}\right)\Delta z$	$z_{23} = \frac{h_2^\circ(\alpha_{13}-h_1^\circ)}{(\alpha_{13}-1)(\alpha_{13}-\alpha_{12})}\Delta z$
$\tau_{23} = \frac{\alpha_{12}\alpha_{13}(\alpha_{13}-h_1^\circ)}{h_1^\circ h_2^\circ(\alpha_{13}-1)(\alpha_{13}-\alpha_{12})}\Delta z$	$\tau_{23} = \frac{\alpha_{13}(\alpha_{13}-h_1^\circ)}{(\alpha_{13}-1)(\alpha_{13}-\alpha_{12})}\Delta z$
Multicomponent separations	
$k = 2,\ldots,n$: $z_{1k} = \frac{\alpha_{1n}}{\alpha_{1n}-1}\prod_{i=k}^{n-1}\left(\frac{\alpha_{1i}(h_i^\circ-1)}{h_i^\circ(\alpha_{1i}-1)}\right)\Delta z$	$z_{1k} = \frac{h_1^\circ}{\alpha_{1n}-1)}\prod_{i=2}^{k-1}\left(\frac{h_i^\circ}{\alpha_{1i}}\right)\prod_{i=k}^{n-1}\left(\frac{h_i^\circ-1}{\alpha_{1i}-1}\right)\Delta z$
$\tau_{1k} = \frac{1}{\alpha_{1n}-1}\prod_{i=2}^{n}\left(\frac{\alpha_{1i}}{h_{i-1}^\circ}\right)\prod_{i=k}^{n-1}\left(\frac{h_i^\circ-1}{\alpha_{1i}-1}\right)\Delta z$	$\tau_{1k} = \left[1 + \frac{1}{\alpha_{1n}-1}\prod_{i=k}^{n-1}\left(\frac{h_i^\circ-1}{\alpha_{1i}-1}\right)\right]\Delta z$
$j = 1,\ldots,n-1$: $z_{jn} = \left[1 + \frac{\alpha_{1j}}{\alpha_{1n}-\alpha_{1j}}\prod_{i=1}^{j-1}\left(\frac{\alpha_{1i}(\alpha_{1n}-h_i^\circ)}{h_i^\circ(\alpha_{1n}-\alpha_{1i})}\right)\right]\Delta z$	$z_{jn} = \frac{h_j^\circ}{\alpha_{1n}-\alpha_{1j}}\prod_{i=1}^{j-1}\left(\frac{\alpha_{1n}-h_i^\circ}{\alpha_{1n}-\alpha_{1i}}\right)\Delta z$
$\tau_{jn} = \frac{1}{\alpha_{1n}-\alpha_{1j}}\prod_{i=2}^{n}\left(\frac{\alpha_{1i}}{h^\circ{}_{i-1}}\right)\prod_{i=1}^{j-1}\left(\frac{\alpha_{1n}-h_i^\circ}{\alpha_{n1}-\alpha_{1i}}\right)\Delta z$	$\tau_{jn} = \frac{\alpha_{1n}}{\alpha_{1n}-\alpha_{1j}}\prod_{i=1}^{j-1}\left(\frac{\alpha_{1n}-h_i^\circ}{\alpha_{1n}-\alpha_{1i}}\right)\Delta z$
$j = 1,\ldots,n-1$; $k = 2,\ldots,n$; $j<k$: $z_{jk} = \frac{\alpha_{1j}\alpha_{1k}}{\alpha_{1k}-\alpha_{1j}}\left[\left(\frac{1}{\alpha_{1j}} - \frac{1}{h_k^\circ}\right)z_{j,k+1} + \left(\frac{1}{h_{j-1}^\circ} - \frac{1}{\alpha_{1k}}\right)z_{j-1,k} - \left(\frac{1}{h_{j-1}^\circ} - \frac{1}{h_k^\circ}\right)z_{j-1,k+1}\right]$	
$\tau_{jk} = \frac{1}{\alpha_{1k}-\alpha_{1j}}\left[(h_k^\circ-\alpha_{1j})\tau_{j,k+1} + (\alpha_{1k}-h_{j-1}^\circ)\tau_{j-1,k} - (h_k^\circ-h_{j-1}^\circ)\tau_{j-1,k+1}\right]$	

Δz = width of rare-earth band in (z,τ) diagram, measured long line of constant τ [for calculation, s
eqn. (29)]; $\alpha_{23} \equiv y_2x_3/x_2y_3 = \alpha_{12}/\alpha_{23}$.

in Fig. 5. In general, the latter type of operation requires a smaller column length but a longer adjusted time for resolution of any given pair of species. Also, the "critical" pair, *i.e.*, that with the longest resolution distance or time, is not necessarily the same for the two types of operation.

For binary and ternary separations the formulas in Table I are explicit in terms of the initial composition of the mixture or its H-function roots, which are readily calculated from the composition by eqn. (13). For separations of higher order, explicit formulas can be given but are impractically lengthy; here Table I only lists those for resolution from species 1 and from species n and gives a recursion formula for calculating z_{jk} (or τ_{jk}) from previously calculated $z_{j-1,k+1}$, $z_{j-1,k}$, and $z_{j,k+1}$ (or corresponding τ values). The equations for the resolution distances in binary and ternary separations are identical with, or equivalent to, those given by SILLÉN[5] and SPEDDING, POWELL *et al.*[4,6-9], although the implicit ternary equations of the latter appear more complex since they lack the economy provided by the H-function roots. (All but the last of these publications, ref. 9, were confined to development of a uniform initial band.)

The initial condition in development of a uniform band calls for a comment. The formulas in Table I are calculated with the premise that no development takes place at any location z prior to that location's zero of adjusted time. That is, development at any z is presumed to start with a time lag z/u_0 relative to the top of the bed (see eqn. (3), solved for t at $\tau = 0$). This time lag is exactly the time needed for a nonsorbable agent to travel from the top to the location z. Accordingly, the premise is geared to operation with a column initially free of any development agent and with development by an agent essentially excluded by the ion exchanger. This corresponds closely to the conditions in practical separations.

Another point needing consideration is that the composition of the original rare-earth mixture provides the initial values $y_1^\circ, \ldots, y_n^\circ$ in development of a uniform presorbed band, but provides the influent values $x_1^\circ, \ldots, x_n^\circ$ in operation with chelation prior to loading. In the first case, the mixture is sorbed nonselectively in the absence of the chelating agent to give an ion-exchanger composition equal to that of the original mixture; as the front of the chelating anion penetrates the band at $\tau = 0$, slight and selective desorption occurs, to give a liquid-phase composition in equilibrium with, and differing from, the essentially unchanged ion-exchanger composition. In contrast, in the second case, the mixture enters the column at its composition $x_1^\circ, \ldots, x_n^\circ$ with the chelating agent providing selective sorption, so that an ion-exchanger composition in equilibrium with, and differing from, this liquid-phase composition is established at the top of the bed. Accordingly, when calculating the set of h_i° from the known composition of the original mixture, this composition should be taken as $y_1^\circ, \ldots, y_n^\circ$ in development of a uniform initial band, and as $x_1^\circ, \ldots, x_n^\circ$ in operation with chelation prior to loading.

The iterative calculation of the resolution distances and times for mixtures with many components, although straightforward, is lengthy if a computer is not available. However, if the establishment of safe design limits is sufficient, the following inequalities can be used. For development of a uniform initial band:

$$z_{jk} < \frac{1/a_{1j}}{1/a_{1j} - 1/a_{1k}} \Delta z, \qquad \tau_{jk} < \frac{1/h_j^\circ}{1/a_{1j} - 1/a_{1k}} \prod_{i=j+1}^{k-1} \left(\frac{a_{1i}}{h_i^\circ}\right) \Delta z \tag{24}$$

and for operation with chelation prior to loading:

$$z_{jk} < \frac{h_j^\circ}{a_{1k} - a_{1j}} \prod_{i=j+1}^{k-1} \left(\frac{h_i^\circ}{a_{1i}}\right) \Delta z, \qquad \tau_{jk} < \frac{a_{1k}}{a_{1k} - a_{1j}} \Delta z \tag{25}$$

[The right-hand sides of these inequalities are calculated with constant values of the velocities of Δh_j and Δh_k equalling the actual values at the zone jk, and therefore constitute upper limits because the actual velocity difference is larger initially and decreases with every crossing of other trajectories (see Fig. 6).]

The equations for the two types of operation reflect certain symmetry properties, more fully discussed in the original theory[10]: the equations for one type can be obtained from those of the other by interchange of x and y and of z and τ, replacement of u, h, and α by their reciprocals, and change of the indices i for the species to $n+1-i$ and for roots to $n-i$.

Notation in the original theory

A slightly different notation has been used here than in the original theory[10], where, to be consistent with the treatment of other kinds of operation, the development ion is species 1, the species of the mixture are 2, . . ., $n-1$, and the retaining ion is n. An m-component separation then appears as an $(m+2)$-component problem and,

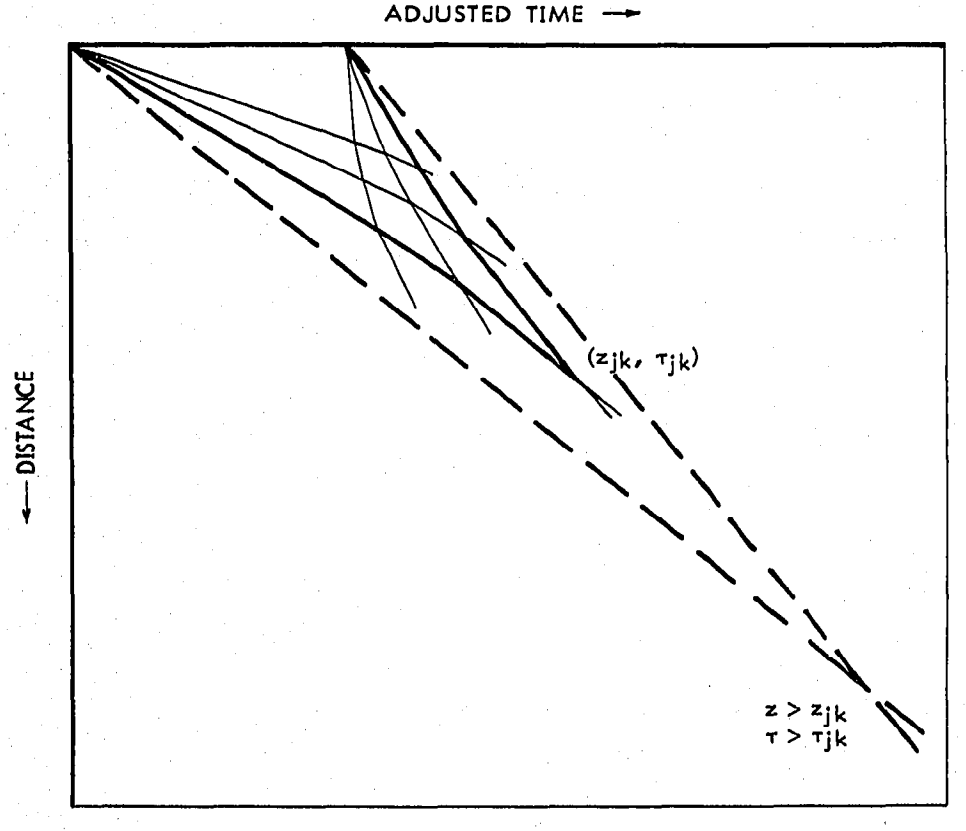

Fig. 6. Calculation of upper limits of resolution distances and times. Solid lines are actual trajectories; broken lines are fictitious linear trajectories used to calculate inequalities (see eqn. 25).

compared with the present treatment, all roots and separation factors (now relative to the development ion) are larger by a factor equalling the separation factor of the development ion and the first ion of the mixture. The invariance to the properties of the development and retaining ions and the attendant possibility of simplifying the notation as done here are discussed in the original.

COMPUTATION FROM OPERATING VARIABLES

The theory outlined above and the computer program RAREARTH[11] are in terms of normalized and adjusted variables. Practical application will require conversion from and to actual physical variables such as volumetric flow rate, column properties, ion-exchange capacity, true distances and times for resolution, etc.

In order to calculate normalized resolution distances and times (Z and T, in units of band width Δz) as well as adjusted boundary velocities u_{Δ} and compositions $x_1, \ldots x_n$ or $y_1, \ldots, y_n$ in the transient pattern, either by hand or with the program RAREARTH, only the separation factors α_{1i} and the fractional rare-earth concentrations in the original mixture are needed. As has been discussed by POWELL AND SPEDDING[4], the separation factors in rare-earth separations by ion exchange are essentially given by the ratios of the stability constants of the complexes formed with the development agent, stronger complexing resulting in lesser affinity for the resin. At least for standard development agents such as ethylenediaminetetraacetic acid (EDTA), the separation factors can thus be calculated from tabulated stability constants*. The fractional rare-earth concentrations in the original mixture are taken as $y_1^\circ, \ldots, y_n^\circ$ in development of a uniformly loaded initial band, and as $x_1^\circ, \ldots, x_n^\circ$ in operation with chelation prior to loading.

Because ion exchange with dilute solutions is essentially stoichiometric and because the exchange at the front and rear of the rare-earth band is complete, *i.e.*, involves complete conversion of the resin to and from the rare-earth form, the total concentration (in mequiv./cm³ liquid phase) is the same in the influent (development agent), within the band, and in the effluent. The conversion of fractional liquid-phase concentrations x_i in the rare-earth band or effluent into actual concentrations c_i (in mequiv./cm³ liquid phase) thus is

$$c_i = c\, x_i \qquad \text{(mequiv./cm}^3\text{ liquid phase)} \tag{26}$$

where c is the concentration of the development agent (in these units). The conversion to mequiv./cm³ of column requires multiplication with the fractional intraparticle void volume, ε:

$$C = \varepsilon c \qquad \text{(mequiv./cm}^3\text{ column)} \tag{27}$$

The ion-exchange capacity (in mequiv./cm³ of column) can be used directly as the total concentration, $\bar{C}$, of rare earths in the ion exchanger. The conversion of the fractional concentrations y_i to any desired units then is obvious.

The conversion of the respective normalized variables to true resolution distances and times and true boundary velocities requires, in addition to C and $\bar{C}$, a knowledge of the linear flow rate, u_0, and the (adjusted) band width Δz. The linear flow rate is the

* With the possible exception of yttrium, for which the separation factor may have to be determined experimentally.

volumetric flow rate $\dot{V}$ (in cm³/sec) divided by the cross-sectional area not occupied by the resin:

$$u_0 = \dot{V}/\varepsilon S \qquad \text{(cm/sec)} \tag{28}$$

where S is the cross-sectional area of the column (in cm²). The quantity Δz is the width of the rare-earth band measured along any line of constant τ in the distance-time diagram. The true width (*i.e.*, measured along a line of constant true time, t) of the band equals the total rare-earth charge, Q (in mequiv.), divided by the overall concentration $\bar{C} + C$ (total number of mequiv. per cm³ column) and the cross-sectional area, S. Conversion with eqn. (3) shows that the width along a line of constant τ then is

$$\Delta z = Q/\bar{C}S \qquad \text{(cm)} \tag{29}$$

The normalized resolution distances $Z \equiv z/\Delta z$ and $T \equiv \tau/\Delta z$, calculated by hand or obtained as output of the program RAREARTH, can now be converted into true distances and times. For distances, from eqn. (29),

$$z = \Delta z\, Z = QZ/\bar{C}S \qquad \text{(cm)} \tag{30}$$

and for times, with eqns. (3) and (27) to (30)

$$t = \frac{1}{u_0}\left(\frac{\bar{C}}{C}\tau + z\right) = \frac{\varepsilon S\,\Delta z}{\dot{V}}\left(\frac{\bar{C}}{\varepsilon c}T + Z\right) = \frac{\varepsilon Q}{\dot{V}}\left(\frac{T}{\varepsilon c} + \frac{Z}{\bar{C}}\right) \text{ (sec)} \tag{31}$$

Moreover, as can be shown from eqn. (3), the conversion of the adjusted boundary velocities, u_Δ, into true velocities u_Δ is

$$u_\Delta = \frac{u_0}{1 + \bar{C}/Cu_\Delta} = \frac{\dot{V}/\varepsilon S}{1 + \bar{C}/\varepsilon c u_\Delta} \qquad \text{(cm/sec)} \tag{32}$$

A slight complication arises in operation with chelation prior to loading if the flow rate and concentration have different values, u_0' and C' (corresponding to $\dot{V}'$ and c'), during loading than during development. The calculation of the normalized variables (x_t, y_t, u_Δ, Z, T) is not affected, but some of the conversions to true physical variables are. The true time for loading will be

$$\Delta t' = Q/c'\dot{V}' \qquad \text{(sec)} \tag{33}$$

The conversion from adjusted or normalized time to true time (counted from the start of loading) then is

for $t \leq \Delta t'$ (corresponding to $T \leqslant 1 - \varepsilon c' Z/\bar{C}$)

$$t = \frac{(\bar{C}/C')\tau + z}{u_0'} = \frac{\varepsilon Q}{\dot{V}'}\left(\frac{T}{\varepsilon c'} + \frac{Z}{\bar{C}}\right)$$

for $\Delta t' \leq t \leq \Delta t' + \dfrac{z}{u_0}$ (corresponding to $1 - \varepsilon c' Z/\bar{C} \leq T \leq 1$)

$$t = \Delta t' + \frac{z - (\bar{C}/C')\,(\Delta z - \tau)}{u_0} = Q\left[\frac{1}{c'\dot{V}'} + \frac{\varepsilon}{\dot{V}}\left(\frac{Z}{\bar{C}} - \frac{1-T}{\varepsilon c'}\right)\right] \tag{34}$$

for $t \geq \Delta t' + \frac{z}{u_0}$ (corresponding to $T \geq 1$)

$$t = \Delta t' + \frac{z + (\bar{C}/C)(\tau - \Delta z)}{u_0} = Q\left[\frac{1}{c'\dot{V}'} + \frac{\varepsilon}{\dot{V}}\left(\frac{Z}{\bar{C}} + \frac{T-1}{\varepsilon c}\right)\right]$$

In addition, the conversions to true velocities and concentrations are affected as follows: for $t < \Delta t'$ (corresponding to $T < 1 - \varepsilon c' Z/\bar{C}$), u_0' (or $\dot{V}'$) is to be substituted for u_0 (or $\dot{V}$) in eqn. (32), and for $t < \Delta t' + z/u_0$ (corresponding to $T < 1$), c' and C' are to be substituted for c and C, respectively, in eqns. (26) and (32).

The relatively complex conversion to true time by eqns. (34) is a consequence of the fact that a flow-rate variation is instantaneously propagated through the column, the liquid being virtually incompressible, whereas a concentration variation in the liquid is propagated only at the rate of liquid-phase flow (assuming that the concentration $\bar{C}$ in the ion exchanger is not appreciably changed). As is illustrated in Fig. 7, the flow rate is u_0' to the left of the line $t = \Delta t'$, and is u_0 to the right of this line, while the concentration is C' to the left of the line $t = \Delta t' + z/u_0$ (which is also the line $T = 1$ and $\tau = \Delta z$), and is C to the right of this line. This leads to the three regions, separated by the two lines, and each covered by one of the three eqns. (34). (For

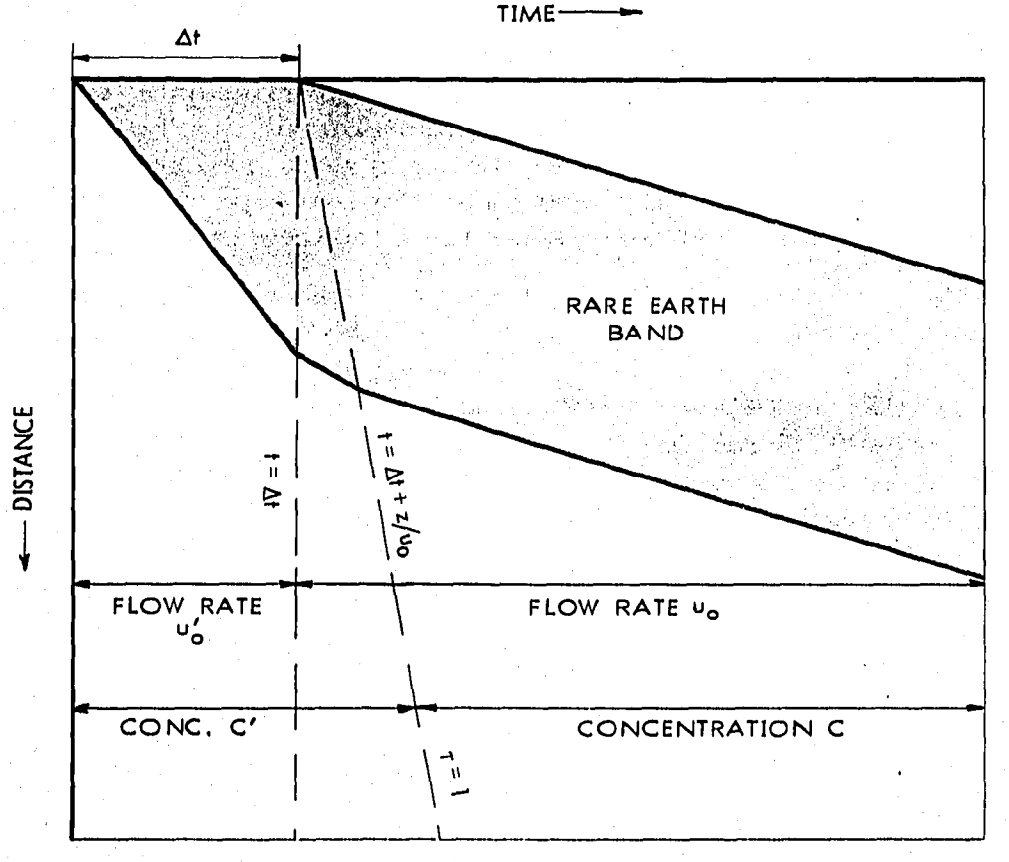

Fig. 7. Chelate loading with different flow rate and concentration (schematic). Changes in slope of band front correspond to loading with flow rate and concentration both twice as high as for development.

clarity, Fig. 7 greatly exaggerates the angle between the lines $t = \Delta t'$ and $t = \Delta t' + z/u_0$.)

An unexpected result is that the true distances (*e.g.*, of resolution) are invariant to changes of flow rate and concentration, since the conversion factor Δz, according to eqn. (29), is independent of these variables. This holds for development of a uniform initial band as well*.

It has been tacitly implied above that the separation factors are not altered by the concentration variation. If they are, an exact calculation, while entirely feasible, becomes quite complex. The computation must then be carried to $\tau = \Delta z$ (corresponding to $T = 1$) with the separation factors pertaining to c', and the composition profile along $\tau = \Delta z$ must then be used as the initial condition for a new calculation with the factors pertaining to c. In general, all boundaries existing at $\tau = \Delta z$, being coherent under the old set of separation factors, will be noncoherent under the new set and will therefore each give rise to a new set of coherent boundaries. This complication exceeds the faculties of the RAREARTH program. Fortunately, the actual concentration dependence of the separation factors of the rare earths is usually not larger than the uncertainty of their measurement, except possibly for lanthanide–yttrium systems. Also, the design is usually dictated by one of the longer resolution distances and times, and these are not much affected by somewhat different separation factors during loading: for species hard to separate, the loading time is but a small fraction of the resolution time and gives very little segregation. For most practical purposes, different separation factors during loading can therefore by ignored.

Another complication not covered here arises if one or several front or rear portions of the incompletely developed band are cut off at some intermediate stage or stages. Boundary trajectories that lead into the discarded portion will then be shifted, at the cut-off distance, to the cut-off point without change in slope, and none of the transient compositions will be altered. The detailed theory for this type of operation, which is of some practical importance, will be presented in a separate publication.

A PRACTICAL EXAMPLE

The practical application of the theory will be illustrated by the calculations for an ion-exchange separation of the rare earths of euxenite by displacement development with ethylenediaminetetraacetic acid (EDTA). A typical fractional composition of the fifteen rare earths of euxenite, a mineral rich in the yttrium earths, is shown in Table II. Table II also lists the separation factors relative to lanthanum (species 1) in the presence of EDTA as calculated from the EDTA stability constants given by WHEELWRIGHT *et al.*[13].

---

* The independence in the range $C \ll \bar{C}$ is, of course, well known from simpler theories. What is shown here is that it extends beyond this range. A compensation of effects is involved. As is known from general chromatographic theory, the separation efficiency lessens with increasing mobile-phase concentration because the relative migration rates of the molecules of the species become more similar (*e.g.*, see ref. 12). In the present case, the numerical values of the resolution distances expressed in units of band length (at constant true time, as used by POWELL *et al.*) indeed increase, but this turns out to be compensated by the shorter length of the band, requiring lesser distances of relocation within the band upon separation, so that the true distances in cm are invariant.

TABLE II

TYPICAL RARE-EARTH COMPOSITION OF EUXENITE AND SEPARATION FACTORS OF EDTA COMPLEXES

Index number	*Element*	*Mole fraction*	*Separation factor* α_{it}
1	Lanthanum	0.006	(1.000)
2	Cerium	0.015	4.68
3	Praseodymium	0.002	10.72
4	Neodymium	0.008	21.88
5	Samarium	0.010	67.61
6	Europium	0.001	93.33
7	Gadolinium	0.035	95.50
8	Terbium	0.016	457.1
9	Yttrium	0.622	691.8
10	Dysprosium	0.095	1,074
11	Holmium	0.035	3,890
12	Erbium	0.090	6,761
13	Thulium	0.015	22,380
14	Ytterbium	0.042	46,770
15	Lutetium	0.008	85,110

For a preparative separation on pilot-plant scale with a general-purpose strong-acid cation-exchange resin, realistic operating variables would be about as follows:

Amount of rare earths	$Q = 20{,}000$ mequiv.
Cross-sectional area of column	$S = 100$ cm^2
Fractional intraparticle void volume	$\varepsilon = 0.4$
Ion-exchange capacity	$\bar{C} = 2.0$ mequiv./cm^3 column
Concentration of development agent	$c = 0.10$ mequiv./cm^3 solution
Volumetric flow rate	$\dot{V} = 2.0$ cm^3/sec

Under these conditions, the band width is 100 cm. (Because $c \ll \bar{C}$, there is virtually no difference between the widths measured along lines of constant t and of constant τ, the "adjustment" of τ by $-z$ in eqn. (3) being negligible.) The time required to displace the band by a distance equal to its own length is $\Delta t = Q/c\dot{V} = 100{,}000$ sec $= 27.8$ h.

Distance–time diagrams for development of a uniformly loaded initial band and for operation with chelation prior to loading, calculated with the program RAREARTH from the data in Table II, are shown in Figs. 8 and 9. Scales of true distance and time have been added in accordance with the operating conditions listed above. For operation with prior chelation, the true-time scale presumes that the concentration and flow rate are the same for loading as for development. For reasons of scale, the diagrams do not extend to the point of resolution of gadolinium from europium, at $Z = 2.644$, $T = 2.601$ for development of a uniform initial band, and at $Z = 1.661$, $T = 2.619$ for operation with prior chelation.

A comparison of the distance–time diagrams for the two types of operation is instructive. In general, development of a uniform initial band requires longer distances but shorter times for resolution. (It should be noted, however, that the time required for loading the initial band is not included!) Development of a uniform band tends to give long resolution distances particularly for the species of low affinity for the resin (*i.e.*, species with a high index number), and operation with prior chelation tends to

give long resolution times particularly for species with high affinity (low index number). Thus, there is incentive to switch from the conventional development of a uniform band to chelated loading if excessive column length is required to resolve a critical pair of low-affinity species.

Another feature that comes out clearly in the example in Figs. 8 and 9 is that resolution of a major component from its neighbors tends to require long distances and times even if the respective separation factors are favorable. Thus resolution of the main component, yttrium (mole fraction 0.622), from terbium in development of a uniform band, and from dysprosium in operation with prior chelation, requires almost as long a distance and time as that of the pair europium–gadolinium, although the separation factors $\alpha_{Tb,Y} = 1.51$ and $\alpha_{Y,Dy} = 1.55$ are significantly larger than $\alpha_{Eu,Gd} = 1.023$.

APPENDIX

Root variations across coherent boundaries

The rule that only one H-function root varies across any coherent boundary can be derived, for displacement development, as follows. According to eqn. (5), the adjusted velocity of a concentration step of an arbitrary species j, regardless of the behavior of other species, is

$$u_{\Delta} = \frac{x_j' - x_j''}{y_j' - y_j''} \tag{A.1}$$

where primes and double primes refer to the two sides of the step. Expressing the x_j and y_j in terms of h_i by means of eqns. (14) and (15) one finds

$$u_{\Delta} = \frac{\prod_{i=1}^{n-1} (h_i' - \alpha_{1j}) - \prod_{i=1}^{n-1} (h_i'' - \alpha_{1j})}{\prod_{\substack{i=1 \\ i \neq j}}^{n} \alpha_{1i} \left\{ \prod_{i=1}^{n-1} [(h_i' - \alpha_{1j})/h_i'] - \prod_{i=1}^{n-1} [(h_i'' - \alpha_{1j})/h_i''] \right\}} \tag{A.2}$$

The condition of coherence is that u_{Δ}, and therefore the right-hand side of eqn. (A.2), will have the same value for all species $j = 1, \ldots, n$. The right-hand side of this equation will meet this condition if, and only if, all features distinguishing j from other species disappear. For this to be the case, all products in the numerator as well as in the denominator must have all factors but one in common. In view of the limits imposed on the root values by condition (9), this requires

$$h_i' = h_i'' \qquad \text{for all } i \neq k \tag{A.3}$$

where k may be any number $1, \ldots, n-1$. That is, all roots but one, h_k, must have the same value on both sides of the step. (At least one root must vary across the step, which otherwise would be nonexistent.) With this restriction, eqn. (A.2) is readily shown to reduce to eqn. (16).

This abbreviated proof presupposes that: (1) the step remains sharp, and (2) equalities $h_i'_{-1} = h_i''$ or $h_i' = h_i''_{-1}$, admitted by condition (9), do not occur.

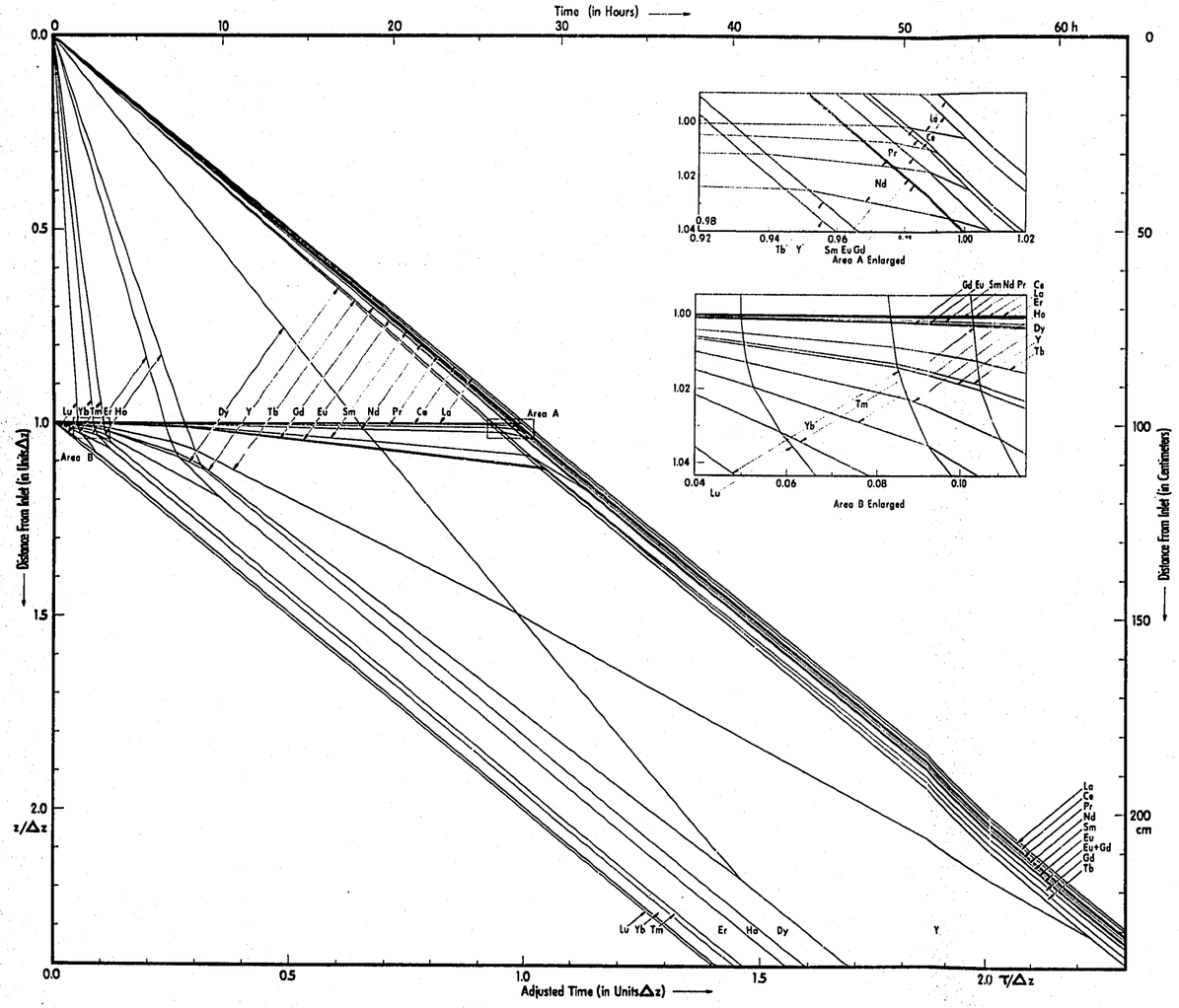

Fig. 8. Distance–time diagram of separation of rare earths of euxenite by development of uniform initial band.

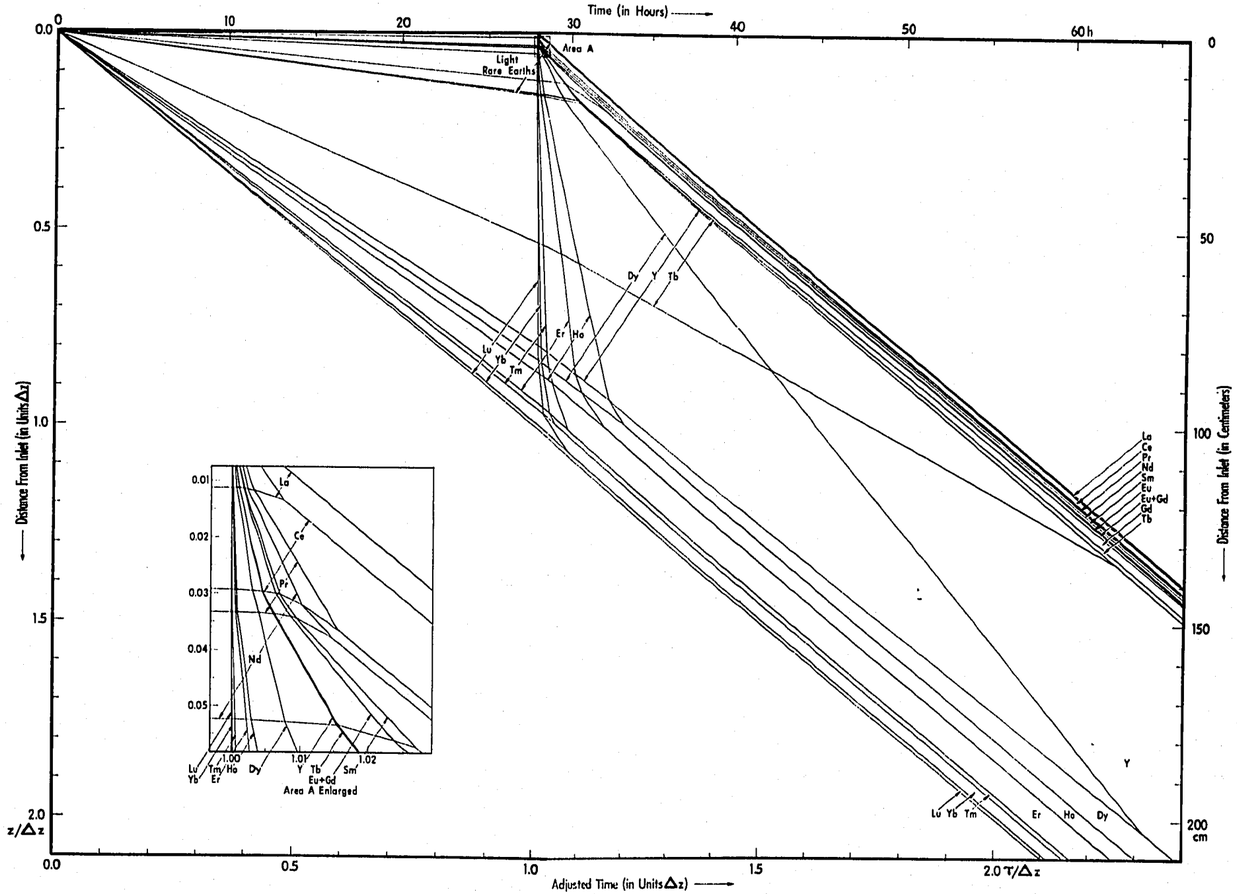

Fig. 9. Distance–time diagram of separation of rare earths of euxenite with chelation prior to loading.

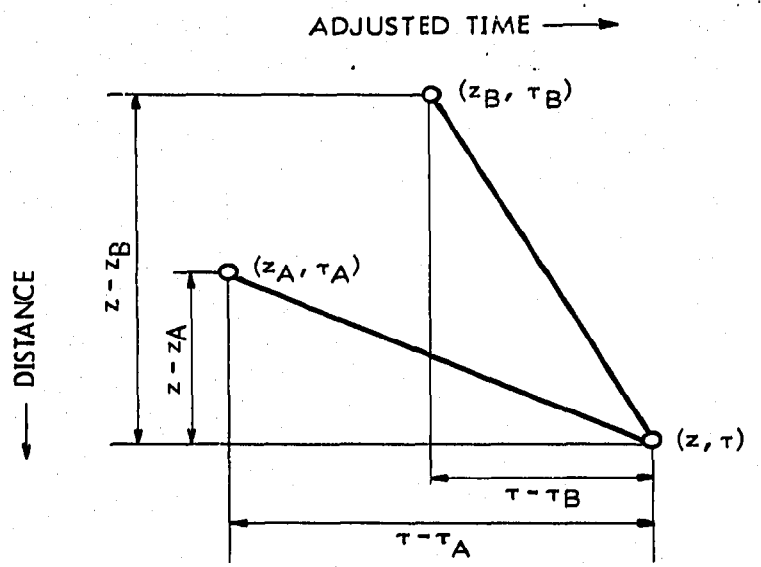

Fig. 10. Trajectories for triangle formula. (From HELFFERICH AND KLEIN[10].)

Calculation of resolution distances and times

The coordinates (z, τ) of intersection of two linear trajectories A and B, with points of origin (z_A, τ_A) and (z_B, τ_B) and slopes u_A and u_B, are calculated as follows. As Fig. 10 shows:

$$u_A = \frac{z - z_A}{\tau - \tau_A} \quad \text{and} \quad u_B = \frac{z - z_B}{\tau - \tau_B} \tag{A.4}$$

Solving for τ and z one finds

$$\tau = \frac{u_B\tau_B - u_A\tau_A - z_B + z_A}{u_B - u_A}$$

$$z = z_A + (\tau - \tau_A)u_A \quad \text{or} \quad z = z_B + (\tau - \tau_B)u_B \tag{A.5}$$

Appropriate values of u_A and u_B can be substituted by means of eqns. (21) and (22). The "triangle formula" (A.5) can then be used to calculate (z_{1n}, τ_{1n}), for which the substitutions are

$$z_A = \Delta z, \quad \tau_A = 0, \quad z_B = 0, \quad \tau_B = 0 \tag{A.6}$$

for development of a uniform initial band, and

$$z_A = 0, \quad \tau_A = 0, \quad z_B = 0, \quad \tau_B = \Delta z \tag{A.7}$$

for operation with chelation before loading. (Note that the band width in the τ direction is also Δz, since the slope of the trajectories of the front and rear boundaries of the band is unity.) Further values (z_{1k}, τ_{1k}) $(k = n-1, \ldots, 2)$ and (z_{jn}, τ_{jn}) $(j = 2, \ldots, n-1)$ are then calculated with the triangle formula as recursion formula, with substitution of the previously calculated $(z_{1,k+1}, \tau_{1,k+1})$ for (z_A, τ_A), or $(z_{j-1,n}, \tau_{j-1,n})$ for (z_B, τ_B). For the simpler expressions in binary and ternary separations, the root or roots can be expressed in terms of x_i or y_i by means of eqns. (12) or (13); this has been done in Table I.

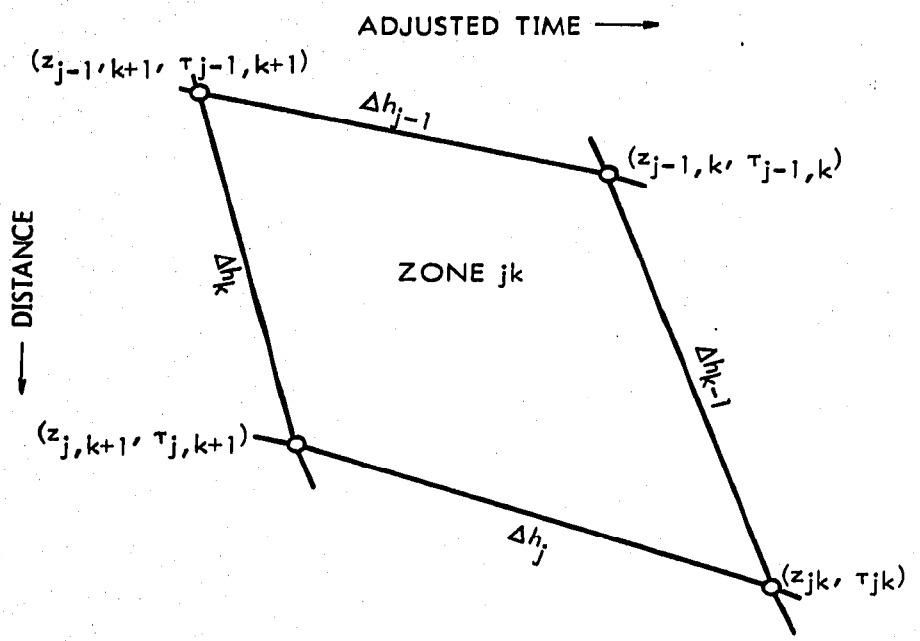

Fig. 11. Trajectories for four-point formula. (From HELFFERICH AND KLEIN[10].)

In principle, the various z_{jk} and τ_{jk} $(2 \leq j < k \leq n-1)$ in separations of four or more species can also be calculated with eqn. (A.5) as recursion formula. However, the "four-point" formulas in Table I, which allow sets of z_{jk} and of τ_{jk} to be generated independently of one another are more convenient. The formula for calculating z_{jk} from $z_{j-1,k}$, $z_{j,k+1}$, is obtained if the equations for the slopes of the four trajectories bounding the zone jk

$$\frac{z_{jk} - z_{j,k+1}}{\tau_{jk} - \tau_{j,k+1}} = \prod_{i=j}^{k-1} \frac{h_i^\circ}{a_{1,i+1}}$$

$$\frac{z_{jk} - z_{j-1,k}}{\tau_{jk} - \tau_{j-1,k}} = \prod_{i=j}^{k-1} \frac{h_i^\circ}{a_{1i}} \qquad \text{(A.8)}$$

$$\frac{z_{j,k+1} - z_{j-1,k+1}}{\tau_{j,k+1} - \tau_{j-1,k+1}} = \prod_{i=j}^{k} \frac{h_i^\circ}{a_{1i}}$$

$$\frac{z_{j-1,k} - z_{j-1,k+1}}{\tau_{j-1,k} - \tau_{j-1,k+1}} = \prod_{i=j-1}^{k-1} \frac{h_i^\circ}{a_{1,i+1}}$$

(see Fig. 11) and the continuity condition

$$(\tau_{jk} - \tau_{j,k+1}) - (\tau_{jk} - \tau_{j-1,k}) + (\tau_{j,k+1} - \tau_{j-1,k+1}) - (\tau_{j-1,k} - \tau_{j-1,k+1}) = 0 \qquad \text{(A.9)}$$

are solved for the five unknowns, that is, for z_{jk} and the four time differences appearing in eqns. (A.8) and (A.9). The derivation of the formula for τ_{jk} is analogous.

SYMBOLS

$A, \bar{A}, B, \bar{B}$	parameters in eqn. (13)
c	concentration of development agent (mequiv./cm³ solution)
c'	total rare-earth concentration during loading of chelated mixture (mequiv./cm³ solution)
c_i	concentration of rare earth i in liquid phase in rare-earth band (mequiv./cm³ liquid phase)
C	total rare-earth concentration in liquid phase in rare-earth band (mequiv./cm³ column)
C'	$= \varepsilon c'$ (mequiv./cm³ column)
$\bar{C}$	ion-exchange capacity (mequiv./cm³ column)
h	argument of the H-function, eqns. (7) and (8)
h_i	i'th root of H-function
n	number of species in original mixture
Q	total amount of rare earths (mequiv.)
S	cross-sectional area of column (cm²)
t	time (sec)
T	$= \tau/\Delta z$
u_0	linear flow rate (cm/sec)
u_Δ	true velocity of boundary (cm/sec)
u_Δ	adjusted velocity of boundary
$\dot{V}$	volumetric flow rate (cm³/sec)
x_i	fractional liquid-phase concentration of rare earth i
y_i	fractional resin-phase concentration of rare earth i
z	distance from top of bed (cm)
z_{ij}	resolution distance of rare earths i and j cm
Z	$= z/\Delta z$
α_{ij}	separation factor of rare earths i and j cm
τ	adjusted time
τ_{ij}	adjusted resolution time of rare earths i and j cm
$h_i^\circ, x_i^\circ, y_i^\circ$	values of h_i, x_i, y_i in uniform initial band or in chelated mixture being loaded
$u_0', \dot{V}'$	values of u_0 and $\dot{V}$ during loading of chelated mixture
h_i', x_i', y_i'	values of h_i, x_i, y_i on upstream side of boundary
h_i'', x_i'', y_i''	values of h_i, x_i, y_i on downstream side of boundary
$\Delta C_i, \Delta \bar{C}_i, \Delta h_i,$ $\Delta x_i, \Delta y_i$	variation of $C_i, \bar{C}_i, h_i, x_i, y_i$ across boundary
$\Delta t'$	time required for loading of chelated mixture (sec)
Δz	adjusted band width (cm)

REFERENCES

1 F. H. SPEDDING AND J. E. POWELL, in F. C. NACHOD AND J. SCHUBERT (Editors), *Ion Exchange Technology*, Academic Press, New York, 1956, Ch. 15.
2 W. L. SILVERNAIL AND N. J. GOETZINGER, in KIRK-OTHMER, *Rare Earth Elements and Compounds*, in A. STANDEN (Editor), *Encyclopedia of Chemical Technology*, 2nd Ed., Vol. 17, Interscience, New York, 1968, p. 143.
3 F. H. SPEDDING, J. E. POWELL AND E. J. WHEELWRIGHT, *J. Am. Chem. Soc.*, 76 (1954) 2557.

4 J. E. POWELL AND F. H. SPEDDING, *Chem. Eng. Progr., Symp. Ser.*, 55, No. 24, (1959) 101.
5 L. G. SILLÉN, *Arkiv Kemi*, 2 (1950) 477.
6 F. H. SPEDDING, J. E. POWELL AND H. J. SVEC, *J. Am. Chem. Soc.*, 77 (1955) 6125.
7 J. E. POWELL, in L. EYRING (Editor), *Progress in the Science and Technology of Rare Earths*, Vol. 1, Pergamon, Oxford, 1964, p. 62.
8 J. E. POWELL, H. R. BURKHOLDER AND D. B. JAMES, *J. Chromatog.*, 32 (1968) 559.
9 D. B. JAMES, J. E. POWELL AND H. R. BURKHOLDER, *J. Chromatog.*, 35 (1968) 423.
10 F. HELFFERICH AND G. KLEIN, *Multicomponent Chromatography. Theory of Interference*, Marcel Dekker, New York, in press.
11 D. B. JAMES, *Computer Program:* RAREARTH *(FORTRAN IV)*, 1968, available from author.
12 R. KAISER, *Chromatographia*, 2 (1969) 125.
13 E. J. WHEELWRIGHT, F. H. SPEDDING AND G. SCHWARZENBACH, *J. Am. Chem. Soc.*, 75 (1953) 4196.